Journal of the Korean Society of Marine Engineering, Vol. 43, No. 8, pp. 618~624, 2019
J. Korean Soc. of Marine Engineering (JKOSME)
https://doi.org/10.5916/jkosme.2019.43.8.618

ISSN 2234-7925 (Print)
ISSN 2234-8352 (Online)
Original Paper

[ICACE2019] Effect of cooling rate on the corrosion resistance and mechanical property of $AlSi_{10}MnMg$ alloy

Cheolmin Ahn[1] · Eunkyung Lee[†]

(Received September 23, 2019 ; Revised October 29, 2019 ; Accepted October 29, 2019)

Abstract: $AlSi_{10}MnMg$ (AA365) is widely used in automobile parts owing to excellent castability and high corrosion resistance. Heat treatments are used to obtain the highest mechanical property of the alloy. The mechanical and corrosion properties of AA365 aluminum alloy in 0.3 M/L H_2SO_4 and 3.5 wt.% NaCl solution according to the different cooling rates were investigated to understand the effects of cooling rates and the type of heat treatments on the performance of the alloy. The lowest corrosion rates in H_2SO_4 and NaCl, were 1.01 and 53.7 mpy, respectively. They were investigated when the specimen treated T4 and cooled at the fastest cooling rate at 9000 K/min after each step among all the cooling rates. It was revealed that the fewer amount of detrimental needle-shaped β-Al_5FeSi phases on corrosion property can be suppressed by the fast cooling rates. With respect to the mechanical property of AA365 alloy, the mechanical strengths of T4 heat-treated alloy cooled at 9000 K/min increased by 76.6 MPa of the ultimate tensile strength and 49.8 MPa of the yield strength more than the alloy cooled at 16 K/min. The mechanical strengths of T6 heat-treated AA365 alloy strengthened mean 11 MPa of the tensile strength and 16 MPa of the yield strength rather than the only solution-treated alloys, owing to age hardening.

Keywords: Aluminum alloy, Microstructure, Heat treatment, Corrosion resistance, Mechanical property

1. Introduction

$AlSi_{10}MnMg$, is known as AA365 (Silafont-36), and is the first successful aluminum-silicon alloy with a low iron content for the application of automobile parts owing to its excellent castability, heat treatable to highest elongation and ductility, and very high corrosion resistance **[1][2]**. The morphology, corrosion resistance and other characteristics of aluminum can be affected by the addition of alloying elements by forming different oxide films that have compatible forms **[3]**. In this point of view, there are two key elements concerning alloy development, which are manganese and magnesium. Manganese avoids sticking to the die and forms globulitic intermetallic phases that provide high ductility and magnesium determines the yield strength and ultimate tensile strength of the alloy.

Regarding corrosion resistance of the alloy, precipitates that contain Fe, Mn, and so on., tend to decrease the corrosion resistance of the alloy in corrosive environments. It was revealed in the previous studies that the aluminum precipitate phase, $Al_6(Fe, Mn)$ has more noble potential as compared to aluminum **[4]** and, thereby, the cathodic reactions have been taking place that are responsible for pitting formation in the surrounding alloy matrix **[3]**. The cathodic reaction of oxygen reduction produces hydroxylation, which helps to break the oxide layer near the Fe-containing particles that promotes the pitting formation **[3][5]**. On the contrary, Mg-Si precipitate was reported to have a lower corrosion potential compared to the aluminum matrix **[6]**. In case of moderate heat treatment, β-phase (Al_3Mg_2) precipitates can be formed along the grain boundaries, and it leads to an increase in anodic activity toward dissolution in a corrosive environment **[7][8]**. This phenomenon is known as the main reason for stress corrosion cracking (SCC) occurring at the grain boundaries of aluminum alloys with precipitates of active phases formed during heat treatment **[9]**. In addition, it is revealed that Fe and Mg distribution can be limited through the addition of Mn which can scavenge these elements in the melt leading to improved corrosion performance **[10]**.

† Corresponding Author (ORCID: http://orcid.org/0000-0001-7593-050X): Assistant Professor, Department of Ocean Advanced Materials Convergence Engineering, Korea Maritime & Ocean University, 727, Taejong-ro, Yeongdo-gu, Busan 49112, Korea, E-mail: elee@kmou.ac.kr, Tel: 051-410-4353

1 M.S Candidate, Department of Ocean Advanced Materials Convergence Engineering, Korea Maritime & Ocean University, E-mail: asdf151512@naver.com, Tel: 051-410-4955

AA365 alloy consists of Si, Mn, and Mg, and it was reported that the intermetallic phases can be formed during cooling of the aluminum alloy, which includes β′, β″, B′, β-Al_5FeSi, and Mg_2Si precipitated at 500 ℃ to 650 ℃ in the matrix **[2][11]**. The mechanical properties regrading precipitations and changes of the grain morphology has been widely investigated, but there is a limited amount of information about the evaluation and analysis of the chemical property. In AA365 alloy, in the high-pressure die-casting, various heat treatments are applied for optimized performances. During the heat treatment processes, precipitations and morphology of grains can be changed in the alloy, and each area of the alloy will be applied with various cooling rates according to their design and thickness. Therefore, it is essential to investigate the corrosion properties of the alloy according to different cooling rates after various heat treatments owing to insufficient information on corrosion properties. Furthermore, it is necessary to evaluate the chemical property of the materials in various environments to assess a possibility if the aluminum alloy would endure the acid or corrosive environment.

In the present study, corrosion resistance and mechanical property of AA365 alloy against acid and salt environments were investigated according to the cooling rates after solid solution treatment and artificial aging. The microstructure effect on the corrosion properties was investigated to confirm that the cooling rates after heat treatments affect the precipitate which is related to corrosion performance.

2. Experimental Methods

An as-cast sample of AA365 (Silafont-36) was used to observe as many phase evolutions as possible. The chemical composition of AA365 was measured as Al - 10.6 wt.% Si - 0.7 wt.% Mn - 0.28 wt.% Mg -0.1 wt.% Fe - 0.08 wt.% Ti, whereas the contents of other elements were less than 0.03 wt.% (Ni, Cr, Ga, Sr, V), as measured by a SpectroMaxX Spark Spectrometer. AA365 alloy was employed by the immersion test according to the ASTM G31 standard **[12]**. Before performing any immersion test, all samples were cut into pieces by a cutting machine. These specimens were heat-treated using T4 (solid solution treatment) and T6 (solid solution treatment + artificial aging). The temperature of the solid solution was held at 500 °C for 2 h and the aging was conducted at 200 °C for 2 h. Four different cooling media, i.e., water (9000 K/min), forced air (168 K/min), air (77 K/min), and furnace cooling (16 K/min) were used to cool the specimens after solid solution treatment and four different cooling media, i.e., water (9118 K/min), forced air (38 K/min), air (37 K/min), and furnace cooling (4 K/min) were used to cool the specimens after artificial aging. The cooling rates of the alloy with different cooling media were measured using temperature data acquisition. The collected data were analyzed with the cooling rate (slope) from the initial temperature of 500 °C (solid solution treatment) and 200 °C (artificial aging). For measurement of mechanical properties, tensile testing was performed at a speed of 0.012 mm/min, according to ASTM E8 **[13]** using three replicates for each condition. The entire and gauge length of a subsize tensile specimen were 100 and 25 mm, respectively. All values of the ultimate tensile strength (UTS), yield strength (YS), and tensile strain (E) of the alloy under different cooling conditions were recorded with an average value and standard deviation. With respect to immersion test, all samples were grounded by 400 grit followed by 600 grit abrasive sandpaper with the final dimension of approximately 20 mm x 15 mm x 3 mm. After final treatment of the surface, each sample was ultrasonically cleaned by ethanol for at least 10 min, then stored in a desiccator for 24 h. The weight of five surfaces area of all dried samples were recorded before immersing it into the solutions. Using nail polish, one of the surfaces was covered that directly touched the bottom of the to eliminate the corrosion rate calculation error. The immersion corrosion tests were conducted in two types of solution, 0.3 M/L H_2SO_4 and 3.5 wt.% NaCl solution, to investigate the corrosion resistance in acid and salt environments. The corrosion rate of AA365 alloy was measured by weight loss at 25 °C under one standard atmospheric pressure in 0.3M/L H_2SO_4 and 3.5 wt.% NaCl solution respectively, and the experiment lasting time is 720 h (30 d). To remove the corrosion product of AA365 alloy, they were cleaned by acetone using Ultrasonicator and weighed the mass after fully dried. According to ASTM G1 standard, the alloy after the 3.5 wt.% NaCl immersion test, dilute phosphoric acid (H_3PO_4) solution mixed with chromium trioxide (CrO_3) at 90–100 °C was used to remove the corrosion product for 10 min, and was followed by nitric acid (HNO_3) at 25 °C for 5 min. They also were cleaned ultrasonically in acetone for 10 min and weighed the mass after fully dried **[14]**. Knowing the mass loss after immersion experiment, and the area of five surfaces, we calculated the corrosion rate of A365 alloy. According to ASTM G31, the corrosion rate could be measured by calculating the

weight loss from the following equation **[12][15]**:

$$m\,py = \frac{(K \times W)}{(A \times T \times D)} \quad (1)$$

where corrosion rate is depicted in mils penetration per year (mpy), W is the weight loss in mg, A is the surface area in in^2 (sum of 5 surfaces), T is the immersion time in h, and D is the density in g/cm^3.

3. Results and Discussion

AA365 aluminum alloy was heat-treated using T4 and T6 with different cooling rates to investigate the mechanical and chemical property of the alloy. The cooling rates of each media were 9000 (water), 168 (forced air), 77 (air), 16 K/min (furnace) after solution treatment, and 9118 (water), 38 (forced air), 37 (air), 4 K/min (furnace) after aging treatment, respectively. In **Figure 1** and **Figure 2**, the corrosion behavior of AA365 alloy was presented after the alloys were soaked in 0.3 M/L H_2SO_4 and 3.5 wt.% NaCl solutions, according to ASTM G31 standard.

Figure 1 shows the corrosion rates of AA365 alloy that was heat-treated using T4 and T6 at each different cooling media in 3.5 wt.% NaCl. In **Figure 1**, ST stands for solid solution treatment. For the alloy with a 16 K/min cooling rate after solid solution treatment, the corrosion rate of AA365 alloy pointed at 1.39 mpy, whereas AA365 alloy cooled at 9000 K/min after the solution exhibited the corrosion rate of 1.01 mpy showing a 37.6 % decrease in the corrosion rate by increasing cooling rates. It is because the intermetallic phases were formed on the Al matrix, especially a needle-shaped β-Al_5FeSi phase. The compound was reported to be a very brittle and low bonding with the Al matrix that can cause a fracture with the initiation of cracks **[16]**. Thus, the Fe-intermetallic phases affected the material to be susceptible to the corrosion and mechanical property **[17]**. Furthermore, AA365 alloy cooled slowly that showed larger β-Al_5FeSi phases than the alloys cooled rapidly because the formation of intermetallic compounds can be restricted by the fast cooling media **[2][18][19]**. Regarding the effect of cooling rate in T6 on the corrosion property, the corrosions rate of an AA365 cooled at 9000 K/min after

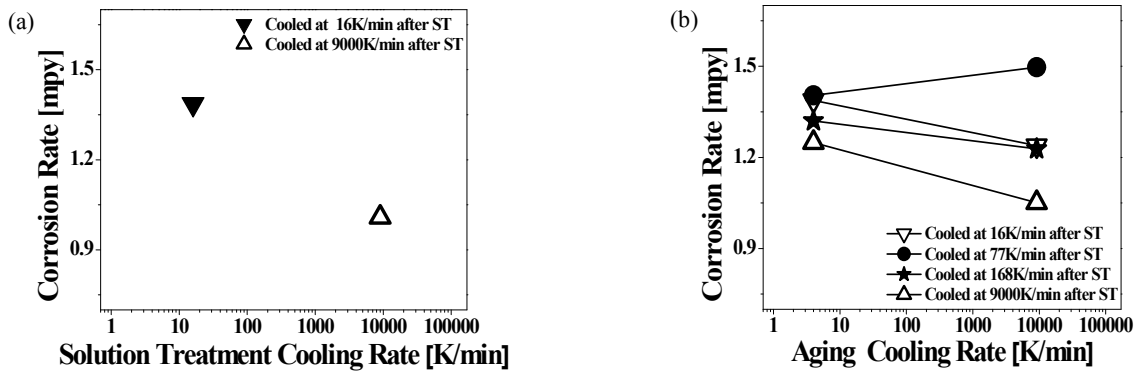

Figure 1: Corrosion rates of AA365 alloy cooled at each different rate after (a) T4 and (b) T6 heat treatment in 3.5 wt% NaCl; ST: Solid Solution

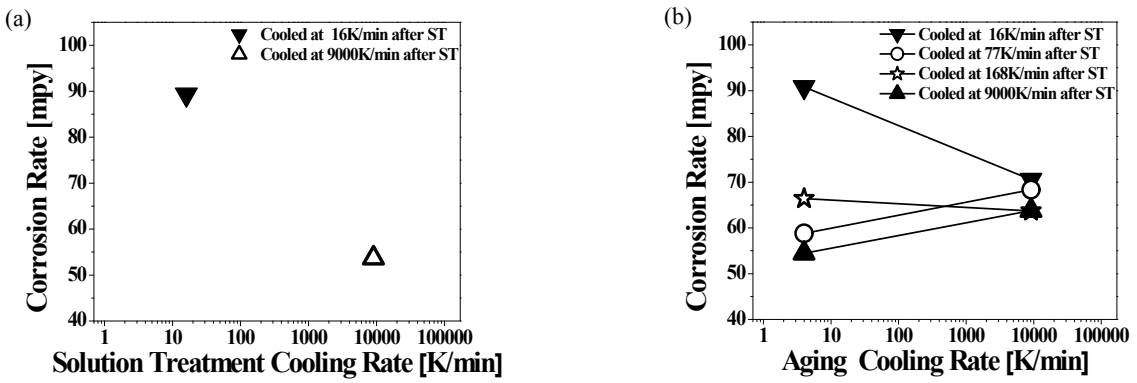

Figure 2: Corrosion rates of AA365 alloy cooled at each different rate after (a) T4 and (b) T6 heat treatment in 0.3M/L H2SO4; ST: Solid Solution Treatment

solution treatment was diminished from 1.24 to 1.05 mpy, and the corrosion rates of the alloys cooled at 168 K/min and 16 K/min after solution treatment were also dwindled from 1.32 and 1.39 mpy to 1.22 and 1.23 mpy, respectively, with increasing the aging cooling rates. However, the AA365 alloy cooled at 77 K/min showed a 0.1 mpy increase by escalating the aging cooling rates. In NaCl, AA365 alloy cooled at 9000 K/min after solid solution treatment exhibited a relatively low corrosion rate value, 1.01 mpy, and the T6 heat-treated alloy cooled at 9000 K/min after solid solution 1.05 mpy and 1.25 mpy, according to the aging cooling rates.

Figure 2 shows the corrosion rates of AA365 alloy, which was heat-treated using T4/T6 and cooled in each different cooling media, in H_2SO_4. The corrosion rate of the alloy cooled at 16 K/min showed 89.3 mpy, and that of the alloy cooled at 9000 K /min was 53.7 mpy, referring to 66.3 % decrease of the corrosion rate that is a bigger value than 37.6 % in NaCl. Although the corrosion potential (E_{corr}) of the aluminum alloy in H_2SO_4 is slightly higher than in NaCl, the corrosion current density (I_{corr}) of H_2SO_4 is approximately 10 times larger than in NaCl. Thus, H_2SO_4 solution has a more detrimental effect on the corrosion of the aluminum alloy rather than NaCl **[20]**. As **Figure 2** shows, the high corrosion resistance can appear by high cooling rates, because the cooling media can diminish or suppress the size of harmful β-Al_5Fe Si phases on the corrosion **[16]**. In the case of T6 heat treatment, the corrosion rates of the alloy cooled at 77 K/min and 9000 K/min after solution treatment increased by approximately 10 mpy, but the alloy cooled 168 K/min after solution treatment showed a 4 mpy decrease of the corrosion rate, following the aging cooling rates. In addition, the corrosion rate of AA365 alloy cooled at 16 K/min decreased to 22.4 % with increasing the aging cooling rates. As a result, the effect of aging treatment and cooling rates influenced the alloy cooled at 16 K/min after solution treatment more than other alloys. It was revealed that some intermetallic phases, which have needle-shaped and random structure, can be precipitated or dissolved at nearly 473 K **[11]**. After aging treatment, the growth of intermetallic compounds can be disturbed by fast cooling rates, but the slow cooling rate can form the large secondary phases, which are deleterious to the corrosion property of the aluminum alloy, on the matrix **[19][21]**. In H_2SO_4, the corrosion rate of an AA365 alloy cooled at 9000 K/min pointed the lowest 53.7 mpy, and that cooled at 9000 K/min after solid solution treatment and aging treatment exhibited relatively low corrosion rate, ranging between 54.5 mpy and 63.8 mpy, according to the aging cooling rates. In **Figure 3**, the microstructures of AA365 aluminum alloy were revealed to investigate the secondary phases in AA365 alloys. A large number of intermetallic phases were found in AA365 alloy, and there were a relatively large size of intermetallic phases at a slow cooling rate, 16 K/min, in **Figure 3 (a)** more than **Figure 3 (c)** of the fast cooling media, 9000 K/min. The sizes of the intermetallic phases were determined by the cooling rates **[16]**. In the SEM images at a magnification of 3,000x, a variety of secondary phases were located on the Al matrix of AA365 alloy. The length of a phase at the center of **Figure 3(b)** was 13.3 μm, and that of a phase in **Figure 3(d)** was 11 μm. The large needle-like particle was a β-Al_5FeSi phase, which is known for a detrimental phase on the corrosion and mechanical property of the material, and it appeared more in the alloy cooled at 16 K/min than 9000 K/min. To investigate the deleterious phase in detail, the chemical elements quantitative maps of intermetallic phases of a T4 heat-treated AA365 alloy were exhibited in **Figure 4**. A needle-shaped phase occurred on the Al matrix, which consists of Al, Si, Fe, and Mn **[22]**.

This compound (β-Al_5FeSi) has been reported to cause cracks and severe corrosion, owing to stress concentration by a plate-like morphology and little coherence with the aluminum matrix, indicating a cathodic behavior **[23]**. With the characteristic of the phases, it was deleterious to the corrosion and mechanical property in AA365 alloys **[21][24]**.

To investigate the effect of T4/T6 and the cooling rate on the mechanical property of AA365 alloy, the characteristics of the alloy were measured. In **Table 1**, ST stands for solid solution heat treatment and AG is aging heat treatment. In addition, E, A, FA, and WQ are a furnace, air, forced air cooling, and water quenching, respectively. In other words, if AA365 alloy cooled in the furnace after solid solution treatment and in water after aging treatment, it marked as ST-E-AG-WQ. As Table 1 lists, the mechanical strengths of T4 heat-treated alloy cooled at 9000 K/min (WQ) increased by 76.6 MPa of the ultimate tensile strength and 49.8 MPa of the yield strength more than the alloy cooled at 16 K/min (E). However, the elongation of AA365 alloy decreased from 6.55 % to 5.01 % with increasing solution treatment cooling rates. It implied that the mechanical strengths of AA365 alloys can be strengthened, but the tensile strain of those may be diminished by fast cooling **[1]**. It showed that the alloy cooled at 9000 K/min after solid solution treatment pointed

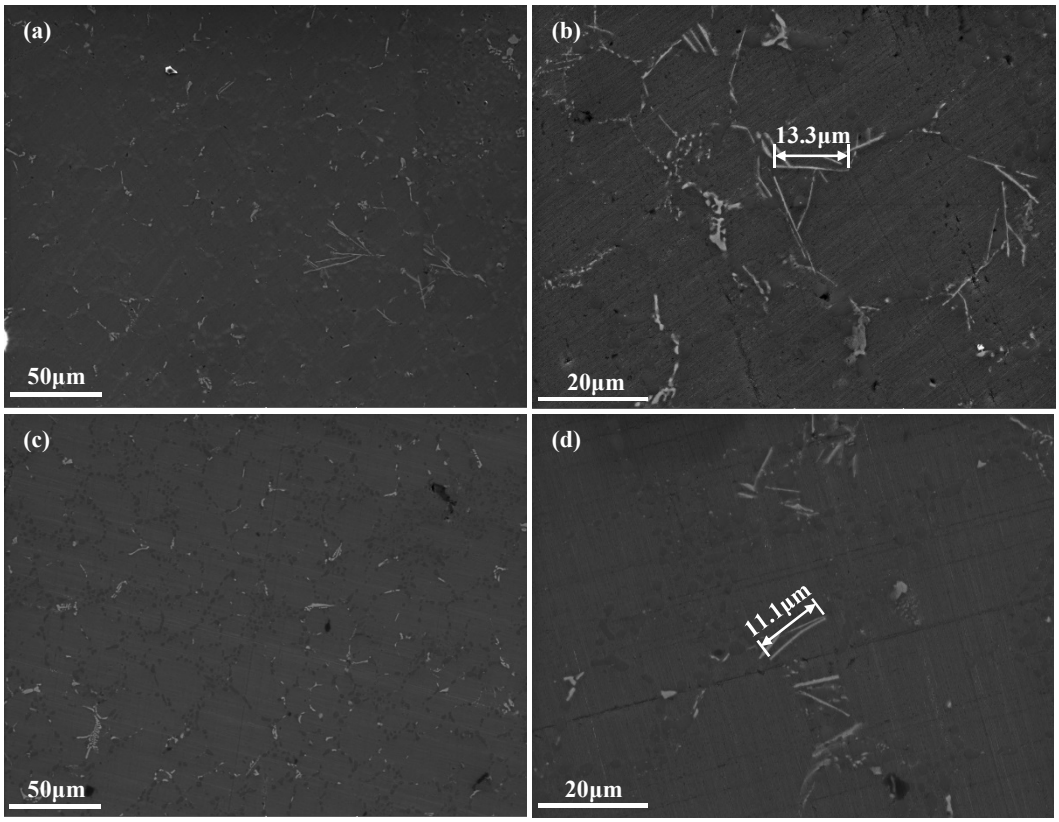

Figure 3: SEM microstructures of AA365 aluminum alloy at various cooling rates: (a) 16 K/min(x1000); (b) 16 K/min(x3000); (c) 9000 K/min (x1000) and (d) 9000 K/min(x3000) after solid solution treatment

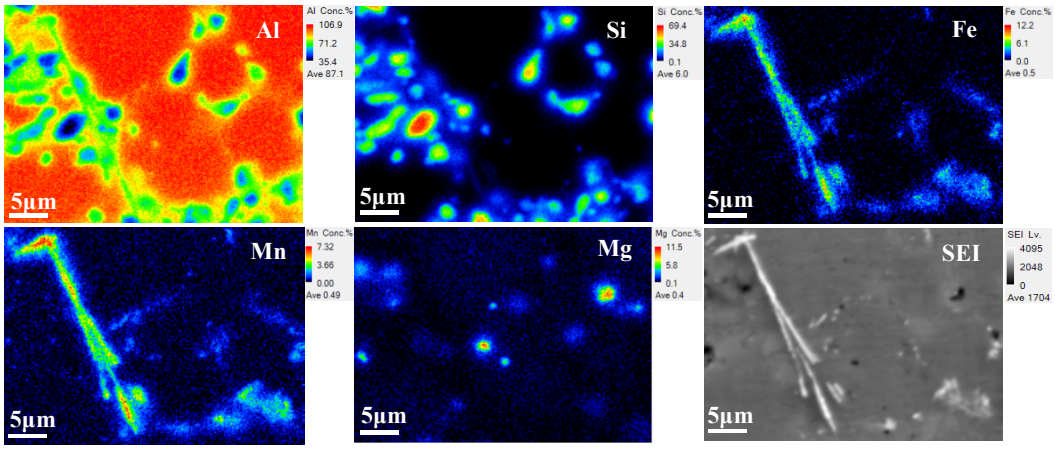

Figure 4: Secondary Electron Image and Chemical elements quantitative maps of AA365 cooled at 16K/min after T4 heat treatment: Al, Si, Fe, Mn, and Mg

at 123.86 MPa in the yield strength. However, the yield strengths of the aging treated alloys that were cooled at 9000 K/min after solid solution treatment, increased by 33, 23.6, 10.6 and 24.3 MPa rather than the values of the T4 treated alloy, according to the aging cooling rates. Similarly, the aging heat treated AA365 alloy reached the higher values of the yield strengths rather than T4 heat-treated AA365 alloy, strengthening by an average of 16.75 %. It was considered that the effect of the age hardening by aging heat treatment affected the mechanical property of AA365 alloys **[25]**.

4. Conclusions

The effects of cooling rates and T4, T6 heat treatment were investigated to understand the mechanical and corrosion property of AA365 aluminum alloy. The corrosion rates of T4 heat-treated AA365 alloy decreased from 89.3 and 1.39 mpy to

Table 1: Mechanical property of AA365 alloy heat-treated in T4 or T6 with different cooling rates; ST: solid solution heat treatment, AG: aging heat treatment, E: furnace cooling, A: air cooling, FA: forced air cooling (fan) and WQ: water quenching

Heat Treatment		Mechanical Property		
		Tensile Strength(MPa)	Yield Strength(MPa)	Tensile Strain(%)
ST-E	None AG	155.1	74.0	6.6
	AG-E	169.6	84.5	9.5
	AG-A	149.6	88.7	5.4
	AG-FA	156.4	85.5	5.5
	AG-WQ	163.0	87.9	7.8
ST-A	None AG	158.6	84.3	5.7
	AG-E	196.1	97.7	7.2
	AG-A	187.5	100.0	6.2
	AG-FA	192.8	102.3	8.0
	AG-WQ	169.4	90.6	3.8
ST-FA	None AG	179.2	95.2	5.3
	AG-E	197.0	110.1	5.8
	AG-A	194.2	118.2	5.4
	AG-FA	177.5	103.1	3.4
	AG-WQ	203.6	106.7	6.7
ST-WQ	None AG	231.7	123.8	5.0
	AG-E	233.7	157.1	3.6
	AG-A	229.6	147.4	3.3
	AG-FA	216.5	134.4	3.5
	AG-WQ	248.5	148.1	5.5

53.7 and 1.01 mpy with increasing the cooling rates in 0.3 M/L H_2SO_4 and 3.5 wt.% NaCl, respectively. This was due to the fewer amounts of β-Al_5FeSi phases that are known as a harmful phase on the corrosion. The deleterious phase can be suppressed by the fast cooling rates, and AA365 alloy cooled at the fast cooling media may have good corrosion resistance with few β-Al_5FeSi phases. In T6, the corrosion rate of AA365 alloy cooled at 16 K/min after solution treatment exhibited the biggest difference of 20.28 mpy in H_2SO_4, and that of AA365 alloy cooled at 9000 K/min after solution treatment showed the biggest difference of 0.2 mpy in NaCl, with increasing the aging cooling rates. As a result, H_2SO_4 solution has a more detrimental effect on the corrosion of the AA365 alloy compared to NaCl. With respect to mechanical property in T4, the fast cooling rate of AA365 alloy, after solution treatment, exhibited the increase of the ultimate tensile strength and yield strength to 231.7 and 123.8 MPa from 155.31 and 74.02 MPa, but the decrease of the elongation to 5.01 % from 6.55 %. As the cooling rate increased, the tensile and yield strength can be increased, while the tensile strain can be decreased. Compared to the alloys heat-treated by solution treatment, the T6 heat-treated AA365 alloy showed the increase in the mechanical property, strengthening the mean by 16 MPa yield strength and 11 MPa tensile strength. The aging heat treatment has a significant effect on the mechanical property of AA365 alloy.

Acknowledgements

This work was supported by the National Research Foundation of Korea (NRF) (NRF-2019R1I1A3A01062863).

Author Contributions

Conceptualization, C. Ahn and E. Lee; Methodology, C. Ahn; Software, C. Ahn; Validation, C. Ahn and E. Lee; Formal Analysis, C. Ahn and E. Lee; Investigation, C. Ahn and E. Lee; Resources, C. Ahn; Data Curation, C. Ahn; Writing—Original Draft, Preparation, C. Ahn; Writing—Review & Editing, E. Lee; Visualization, C. Ahn; Supervision, E. Lee; Project Administration, E. Lee; Funding Acquisition, E. Lee.

References

[1] E. Lee and B. Mishra, “Effect of cooling rate on the mechanical properties of AA365 aluminum alloy heat-treated under T4, T5, and T6 conditions,” International Journal of Metalcasting, vol. 12, no. 3, pp. 449-456, 2018.

[2] E. Lee, C. Walde, and B. Mishra, “Effects of cooling rate on precipitate evolution and residual stresses in Al–Si–Mn–Mg casting alloy,” Metals and Materials International, vol. 24, no. 4, pp. 815-820, 2018.

[3] Z. Szklarska-Smialowska, “Pitting corrosion of aluminum,” Corrosion Science, vol. 41, no. 9, pp. 1743-1767, 1999.

[4] G. A. Gehring Jr and M. Peterson, “Corrosion of 5456-H117 aluminum in high velocity sea water,” Corrosion, vol. 37, no. 4, pp. 232-242, 1981.

[5] E. V. Koroleva, G. E. Thompson, G. Hollrigl, and M. Bloeck, “Surface morphological changes of aluminium alloys in alkaline solution:: effect of second phase material,” Corrosion Science, vol. 41, no. 8, pp. 1475-1495, 1999.

[6] K. Mizuno, A. Nylund, and I. Olefjord, “Surface reactions during pickling of an aluminium–magnesium–silicon alloy in phosphoric acid,” Corrosion Science, vol. 43, no. 2, pp. 381-396, 2001.

[7] M. C. Carroll, P. I. Gouma, G. S. Daehn, and M. J. Mills, “Effects of minor Cu additions on a Zn-modified Al-5083 alloy,” Materials Science and Engineering: A, vol. 319-321, pp. 425-428, 2001.

[8] G. Jones, G. and C. J. Richards, “Metallocene-appended imidazoles displaying virtual planar chirality,” Organometallics, vol. 20, no. 6, pp. 1251-1254, 2001.

[9] M. C. Carroll, P. I. Gouma, M. J. Mills, G. S. Daehn, and B. R. Dunbar, “Effects of Zn additions on the grain boundary precipitation and corrosion of Al-5083,” Scripta Materialia, vol. 42, no. 4, pp. 335-340, 2000.

[10] G. Ballerini, U. Bardi, R. Bignucolo, and G. Ceraolo, “About some corrosion mechanisms of AZ91D magnesium alloy,” Corrosion Science, vol. 47, no. 9, pp. 2173-2184, 2005.

[11] K. Matsuda, S. Ikeno, K. Terayama, H. Matsui, T. Sato, and Y. Uetani, “Comparison of precipitates between excess Si type and balanced-type Al-Mg-Si alloys during continuous heating,” Metallurgical and Materials Transactions A, vol. 36, no. 8, pp. 2007-2012, 2005.

[12] ASTM, Standard Practice for Laboratory Immersion Corrosion Testing of Metals. vol. ASTMG31-12a, West Conshohocken, PA: ASTM International, 2012.

[13] ASTM, Standard Test Methods for Tension Testing of Metallic Materials. vol. E8 / E8M-16a, West Conshohocken, PA: ASTM International, 2016.

[14] ASTM G1-72, Standard Practice for Preparing, Cleaning, and Evaluating Corrosion Test Specimens. 2017.

[15] L. S. Van Delinder, Corrosion Basics-An Introduction., NACE, Houston, Texas, 1984.

[16] J. A. Taylor, “The effect of iron in Al-Si casting alloys,” in 35th Australian Foundry Institute National Conference, Adelaide, South Australia, pp. 148-157, 2004.

[17] X. Cao and J. Campbell, “Morphology of β-Al5FeSi phase in Al-Si cast alloys,” Materials Transactions, vol. 47, no. 5, pp. 1303-1312, 2006.

[18] M. M. Buarzaiga and S. J. Thorpe, “Corrosion behavior of as-cast, silicon carbide particulate-aluminum alloy metal-matrix composites,” Corrosion, vol. 50, no. 3, pp. 176-185, 1994.

[19] J. A. Taylor, “Iron-containing intermetallic phases in Al-Si based casting alloys,” Procedia Materials Science, vol. 1, pp. 19-33, 2012.

[20] H. S. Ryu, T. S. Lim, J. H. Ryu, D. S. Park, and S. H. Hong, “Electrochemical corrosion properties of YSZ coated AA1050 aluminium alloys prepared by aerosol deposition,” Journal of the Korean Ceramic Society, vol. 48, no. 5, pp. 439-446, 2011..

[21] Y. Osawa, S. Takamori, T. Kimura, K. Minagawa, and H. Kakisawa, “Morphology of intermetallic compounds in Al-Si-Fe alloy and its control by ultrasonic vibration,” Materials Transactions, vol. 48, no. 9, pp. 2467-2475, 2007.

[22] S. Ferraro, A. Fabrizi, and G. Timelli, “Evolution of sludge particles in secondary die-cast aluminum alloys as function of Fe, Mn and Cr contents,” Materials Chemistry and Physics, vol. 153, pp. 168-179, 2015.

[23] M. Mahta, M. Emamy, X. Cao, and J. Campbell, Overview of β-Al5FeSi phase in Al-Si alloys, in Materials Science Research Trends, Nova Science Publishers, pp. 251-271, 2008.

[24] R. Arrabal, B. Mingo, A. Pardo, M. Mohedano, E. Matykina, and I. Rodríguez, “Pitting corrosion of rheocast A356 aluminium alloy in 3.5 wt.% NaCl solution,” Corrosion Science, vol. 73, pp. 342-355, 2013.

[25] E. Sjölander and S. Seifeddine, “Artificial ageing of Al–Si–Cu–Mg casting alloys,” Materials Science and Engineering: A, vol. 528, no. 24, pp. 7402-7409, 2011.